The Journal of Immunology

Mitochondrial Reactive Oxygen Species Induces NLRP3-Dependent Lysosomal Damage and Inflammasome Activation

Michelle E. Heid, Peter A. Keyel, Christelle Kamga, Sruti Shiva, Simon C. Watkins and Russell D. Salter

J Immunol 2013; 191:5230-5238; Prepublished online 2 October 2013;
doi: 10.4049/jimmunol.1301490
http://www.jimmunol.org/content/191/10/5230

The Journal of Immunology is published twice each month by
The American Association of Immunologists, Inc.,
1451 Rockville Pike, Suite 650, Rockville, MD 20852

Print ISSN: 0022-1767 Online ISSN: 1550-6606.

Mitochondrial Reactive Oxygen Species Induces NLRP3-Dependent Lysosomal Damage and Inflammasome Activation

Michelle E. Heid,* Peter A. Keyel,* Christelle Kamga,† Sruti Shiva,† Simon C. Watkins,‡ and Russell D. Salter*

The nucleotide-binding oligomerization domain–like receptor family, pyrin domain–containing 3 (NLRP3) inflammasome drives many inflammatory processes and mediates IL-1 family cytokine release. Inflammasome activators typically damage cells and may release lysosomal and mitochondrial products into the cytosol. Macrophages triggered by the NLRP3 inflammasome activator nigericin show reduced mitochondrial function and decreased cellular ATP. Release of mitochondrial reactive oxygen species (ROS) leads to subsequent lysosomal membrane permeabilization (LMP). NLRP3-deficient macrophages show comparable reduced mitochondrial function and ATP loss, but maintain lysosomal acidity, demonstrating that LMP is NLRP3 dependent. A subset of wild-type macrophages undergo subsequent mitochondrial membrane permeabilization and die. Both LMP and mitochondrial membrane permeabilization are inhibited by potassium, scavenging mitochondrial ROS, or NLRP3 deficiency, but are unaffected by cathepsin B or caspase-1 inhibitors. In contrast, IL-1β secretion is ablated by potassium, scavenging mitochondrial ROS, and both cathepsin B and caspase-1 inhibition. These results demonstrate interplay between lysosomes and mitochondria that sustain NLRP3 activation and distinguish cell death from IL-1β release. ***The Journal of Immunology*****, 2013, 191: 5230–5238.**

Inflammasome activation plays an integral part of the innate immune response in host defense and other inflammatory diseases. The nucleotide-binding oligomerization domain–like receptor family, pyrin domain–containing 3 (NLRP3) inflammasome is present in a variety of cells, including macrophages, dendritic cells, neutrophils, T cells, B cells, and some epithelial cells (1). The NLRP3 inflammasome is a protein scaffolding complex consisting of NLRP3, caspase-1, and the adaptor molecule ASC (Pycard) that induces secretion of IL-1 family cytokines, including IL-18 and IL-1β (2, 3). The processing of IL-1β from biologically inactive precursor to the active form requires cleavage by caspase-1, which is recruited to the NLRP3 inflammasome complex by binding ASC. In addition, NLRP3 activation triggers an inflammatory caspase-1–dependent death process termed pyroptosis (4). Whereas IL-1β processing and release require caspase-1 catalytic activity, pyroptosis can be mediated by uncleaved caspase-1 following activation of NLRC4 or AIM2 inflammasomes (5).

Although the exact mechanism of NLRP3 inflammasome activation has remained elusive, a variety of danger-associated molecular patterns and pathogen-associated molecular patterns, including ATP, nigericin, pore-forming toxins, silica crystals, and aluminum hydroxide, have been shown to trigger inflammation through NLRP3 activation (6). The chemical diversity of these stimuli suggests that they may induce a common cellular stress response rather than binding directly to the NLRP3 inflammasome. Potassium efflux from cells is required for NLRP3 activation by almost all stimuli examined, suggesting that compromised membrane integrity is a common feature of this pathway (1).

Several reports attributed the activation of the NLRP3 inflammasome to the leakage of lysosomal contents into the cytosol following phagocytosis of particulate stimuli that could damage their integrity (7, 8). Using inhibitors that blocked inflammasome activation, it was suggested that cathepsin B might be responsible for proteolytically activating NLRP3 inflammasome (7). This process, characterized by the loss of lysosomal contents and acidity, has been termed lysosomal membrane permeabilization (LMP) (9). There remains uncertainty about the generality of this model because not all NLRP3 activators are phagocytosed and disrupt lysosomes directly. Further, it has been suggested that the cathepsin B inhibitor used, CA-074 Me, may not be specific, as RNA interference knockdown and use of cells from cathepsin $B^{-/-}$ mice did not recapitulate CA-074 Me results (9, 10). Alternatively, release of reactive oxygen species (ROS) into the cytosol during LMP could trigger NLRP3 activation, suggested by the observation that NLRP3 inflammasome can be activated by addition of superoxide to macrophage cultures (11). However, inhibition of lysosomal ROS generation with NADPH oxidase (Nox)1–4 knockout mice did not show a corresponding decrease in NLRP3 inflammasome activation (11, 12).

A role for mitochondria as another potential source of ROS has also been explored (11, 13). Mitochondria are sensitive to cellular stress and respond through depolarization of the mitochondrial membrane, ROS release, a decrease in mitochondrial ATP, and reversible opening of the mitochondrial permeability transition

*Department of Immunology, University of Pittsburgh, Pittsburgh, PA 15261; †Department of Pharmacology and Chemical Biology, University of Pittsburgh, Pittsburgh, PA 15261; and ‡Department of Cell Biology, University of Pittsburgh, Pittsburgh, PA 15261

Received for publication June 6, 2013. Accepted for publication September 10, 2013.

This work was supported by National Institutes of Health Grants T32AI089443, T32AI060525, and 5R01AI072083. The work at the Center for Biological Imaging was supported by National Institutes of Health Grant P30CA47904.

Address correspondence and reprint requests to Dr. Russell D. Salter, Department of Immunology, University of Pittsburgh, 200 Lothrop Street, Pittsburgh, PA 15261. E-mail address: rds@pitt.edu

The online version of this article contains supplemental material.

Abbreviations used in this article: BMDM, bone marrow–derived macrophage; cIMDM, complete IMDM; LDH, lactate dehydrogenase; LMP, lysosomal membrane permeabilization; MMP, mitochondrial membrane permeabilization; mtDNA, mitochondrial DNA; NLRP3, nucleotide-binding oligomerization domain–like receptor family, pyrin domain–containing 3; Nox, NADPH oxidase; OCR, oxygen consumption rate; PS, phosphatidylserine; ROS, reactive oxygen species; TLO, tetanolysin O; WT, wild-type.

www.jimmunol.org/cgi/doi/10.4049/jimmunol.1301490

pore. A later marker of mitochondrial damage, mitochondria membrane permeabilization (MMP), can result in the release of additional mitochondrial contents, including cytochrome *c*, and eventual cell death (14, 15).

Recent reports showing that mitochondrial DNA (mtDNA) can activate the NLRP3 inflammasome have further supported a role for mitochondria in inflammasome activation (16). Inhibition of mitophagy promotes the accumulation of dysfunctional mitochondria in cells, and their eventual breakdown was suggested to increase levels of mtDNA in the cytosol (17). A second study showed directly that oxidized mtDNA can activate NLRP3 inflammasome (18).

In this study, we present evidence that NLRP3 inflammasome activation occurs prior to both LMP and MMP. Using a combination of live-cell imaging and biochemical approaches, we demonstrate that prototypical NLRP3 stimuli, the potassium ionophore nigericin, or millimolar concentrations of ATP exert both NLRP3-independent and -dependent effects on macrophages that result in cytokine release and cell death. We present a kinetic model integrating the roles of mitochondria and lysosomes in this process.

Materials and Methods

Bone marrow–derived macrophage preparation

As previously described (19), bone marrow was harvested from the tibiae and femora of wild-type (WT) or NLRP3$^{-/-}$ B6 mice (gifts from Dr. Lisa Borghesi, Dr. Olivera Finn, and Dr. Timothy Billiar). Cells were grown in the presence of 20% FBS (GemCell), 2 mM L-glutamine (Cellgro), 500 U penicillin/500 μg streptomycin (Lonza), 1 mM sodium pyruvate (MP Biomedicals), and 30% L cell supernatant made from culturing L cell fibroblasts (CCL-1 from American Type Culture Collection) for ~6 d. Media of monocytes was replaced after 4 d. Cells were then harvested and grown in IMDM (HyClone) called complete IMDM (cIMDM) when supplemented with 10% FBS, 2 mM L-glutamine, and 500 U penicillin/500 μg streptomycin and were harvested with Cellstripper (Cellgro; Mediatech) for experiments from days 8–25.

Tetanolysin O preparation

Tetanolysin O (TLO; Enzo Life Sciences) was reduced as previously described (19). Serum containing media was washed out prior to the addition of TLO to cells. A total of 100 ng/ml was added in serum-free media to appropriate dishes and incubated at 37˚C for the duration of imaging as indicated.

MTT assay

WT or NLRP3$^{-/-}$ bone marrow–derived macrophages (BMDM) were plated the day before the experiment at 500,000 cells/well in a 12-well tissue-culture plate (Costar) in cIMDM, as described above. Cells were incubated for 4 h with 1 μg/ml LPS (Sigma-Aldrich). A total of 50 mM KCl, 100 or 500 μM Mito-Tempo (Enzo Life Sciences), or 100 μM Ac-YVAD-CMK (Alexis) were added during the last 30 min of LPS treatment and then readded when media was removed, and 1 ml fresh phenol red–free-supplemented IMDM (Life Technologies) was added to the wells. A total of 20 μM nigericin sodium salt (Sigma-Aldrich) or 30 mM ATP (Sigma-Aldrich) was added to the wells and incubated at 37˚C for 5–30 min. After supernatants were removed, cells were washed once with 1× DPBS (Cellgro; Mediatech), and the Vybrant MTT cell proliferation assay kit (Invitrogen/Molecular Probes) was used according to the manufacturer's instructions. Samples were then assayed in duplicate for OD using a PowerWave XS microplate spectrophotometer (BioTek). Percent MTT converted to formazan in the sample was calculated by (mean OD of sample − mean OD of blank)/(mean OD of untreated control − mean OD of blank) × 100. Percent unconverted MTT was graphed.

Lactate dehydrogenase release assay

WT and NLRP3$^{-/-}$ BMDM were treated as described above for the MTT assay. A total of 1% Triton X-100 (Fisher Scientific) was incubated with cells for 5 min as a positive control for complete cell lysis. Supernatants were removed and assayed in duplicate using a lactate dehydrogenase (LDH) cytotoxicity kit (Cayman Chemical) for OD using a PowerWave XS microplate spectrophotometer (BioTek). Percent LDH release was calculated as (mean OD value of sample − mean OD value of blank)/(mean OD value of Triton X-100 control sample − mean OD of blank) × 100.

Quantification of ATP remaining in cell

WT or NLRP3$^{-/-}$ BMDM were treated as described for the LDH assay. Supernatants were removed. Using CellTiter-Glo Luminescent Cell Viability Assay (Promega), ATP levels remaining in the cell lysates were determined using a Berthold Orion microplate luminometer (Berthold Technologies) according to the kit instructions and Simplicity 2.1 software. Results were recorded as a percentage of ATP remaining in cells based on untreated control cells.

Seahorse assay

WT or NLRP3$^{-/-}$ BMDM were plated the night before at 500,000 cells/well in a Seahorse 24-well V7 microplate (Seahorse Bioscience). Cells were LPS primed at 1 μg/ml for 4 h. Media was removed from wells, and cells were incubated in buffered growth media for 1 h after pretreatment with nitrite. A total of 20 μM nigericin was added into wells in unbuffered media prior to inserting the plate into the Seahorse XF24 Extracellular Flux analyzer (Seahorse Bioscience). After 21.5 min of equilibration, media was injected as a control, oligomycin (20 μM) was injected into each well at 48 min, followed by FCCP (75 μM) at 73 min and rotenone (20 μM) at 99 min. Oxygen consumption rate (OCR) was recorded as picomoles per minute. Averages of three wells were taken per data point.

Live-cell microscopy

WT or NLRP3$^{-/-}$ BMDM were plated at 250,000 cells/dish in 35-mm collagen-coated glass-bottom culture dishes (MatTek) the night before the experiment in cIMDM. Media was removed, and cells were LPS primed (1 μg/ml) for 3 to 4 h in fresh media. Inhibitors were added during the last 30 min of LPS priming at 37˚C and added back to the dish in fresh media before imaging following washing out LPS-containing media. YVAD was added at 100 μM, and CA-074 Me (Calbiochem) was added at 100 μM. A total of 2 μM MitoTracker Red CM-H2XRos (Invitrogen), 10 μM TMRM, or 2 μM LysoTracker Green DND-26 (Invitrogen) was added during the last 30 min of LPS priming. A total of 10 μl/ml pSIVA (Imgenex) was added in 1 ml cIMDM two frames after the initiation of imaging after 30-min preincubation. Dishes were imaged on a Nikon A1 inverted microscope (Nikon) with a Plan Fluor 40× objective with an 1.30 numerical aperture or Plan Apo 60× objective with a 1.40 numerical aperture, Photometrics Coolsnap HQ2 or Andor Technology iXon^{EM}+ camera, NikonPiezo driven XYZ stage, and Tokai Hit Environmental chamber. For MitoTracker, LysoTracker, TMRM, and pSIVA, images were captured every 30 s for 1 h. A total of 20 μM nigericin or 3 mM ATP was added 2 min into imaging in 1 ml media. Videos were analyzed using Elements (Nikon) and Microsoft Excel (Microsoft, Redmond, WA).

IL-1β ELISA

WT or NLRP3$^{-/-}$ BMDM were plated at 500,000 cells/well in a 12-well tissue-culture plate the night before. Cells were LPS primed for 4 h and treated as indicated. An IL-1β ELISA was performed as previously described (19). OD values were read at 450 nm with 570 nm background subtraction using a BioTek Powerwave XS Microplate Spectrophotometer and Gen5 Data Analysis Software.

IL-1β Western blot

Lysates and supernatants were collected from 2.0 × 10^6 BMDM after treating cells as indicated in serum-free IMDM. Supernatants were TCA precipitated, and both lysates and supernatants were analyzed for IL-β via Western blot as previously described (19). Western blotting luminal reagent (Santa Cruz Biotechnology) was added before imaging on a Kodak Image Station 4000MM (Molecular Imaging Systems).

Statistical analysis

All data sets were analyzed via a Student two-tailed *t* test unless otherwise noted using GraphPad software (GraphPad). The *p* values were as indicated and considered significant if $p < 0.05$.

Results

NLRP3 inflammasome activation increases sensitivity of BMDM to membrane damage

The NLRP3 inflammasome is present in a variety of immune cells, including macrophages. Due to the robustness of NLRP3 activation in murine BMDM, this system has frequently been employed to

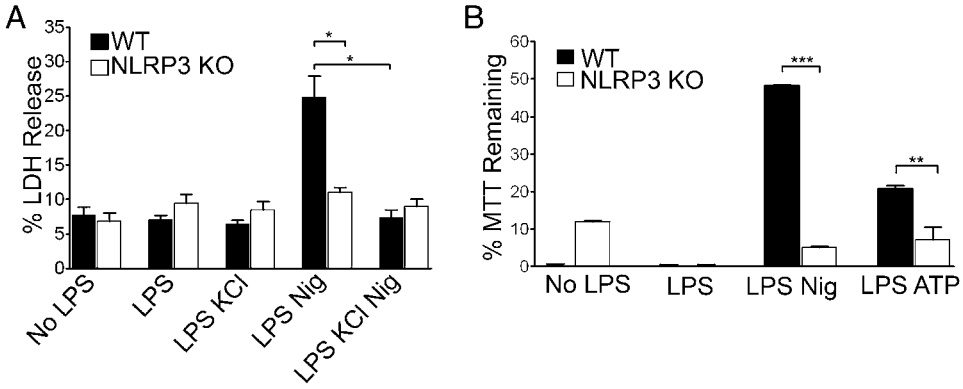

FIGURE 1. NLRP3-dependent cell membrane damage. (**A**) LPS-primed or unprimed WT and NLRP3$^{-/-}$ BMDM were treated with 20 μM nigericin (Nig) or 3 mM ATP for 30 min with or without KCl. LDH release was recorded as the percent released into the supernatant by 5 min of Triton X-100 treatment. LDH assay was allowed to develop for 2 h, and readings were taken as an average of two wells. Error bars represent mean ± SD ($n = 3$; *$p <$ 0.01. LPS Nig WT versus knockout [KO]: $p = 0.009$. WT LPS Nig versus WT LPS Nig KCl: $p = 0.004$). (**B**) Conversion of MTT reagent added to cell lysates was measured as absorbance of the colored product formazan. Data were acquired as the percent of absorbance of each well/absorbance of Triton X-100–treated control cells and graphed as MTT reagent remaining unconverted by mitochondrial reductases. Readings were taken as an average of two wells. Error bars represent mean ± SD ($n = 3$, **$p = 0.0155$. $n = 4$, ***$p < 0.0001$).

examine NLRP3 inflammasome activation and function. BMDM were primed with LPS for 3 to 4 h to upregulate inflammasome components as well as induce the translation of pro–IL-1β, a cytokine that is processed into its active form during NLRP3 inflammasome–dependent caspase-1 activation. Following priming, BMDM from WT C57/BL6 mice were treated with the potassium ionophore nigericin, a prototypical activator of the NLRP3 inflammasome.

To test membrane permeability, LDH was measured in the culture supernatants. Following nigericin treatment, LDH levels were increased in the supernatants of LPS-primed WT BMDM but not LPS-primed NLRP3$^{-/-}$ cells, indicating that the cell membrane integrity had been compromised in the former (Fig. 1A). Pretreatment of WT BMDM with 50 mM KCl to block potassium efflux significantly inhibited release of LDH. Non–LPS-primed or BMDM treated with LPS alone did not release LDH above background levels.

An additional assay of cell viability, the conversion of MTT to formazan, which is carried out by mitochondrial reductases, showed similar results. LPS-primed WT and NLRP3$^{-/-}$ BMDM differed significantly in MTT reduction after nigericin exposure (Fig. 1B). We next tested whether ATP, a second well-characterized stimulator of NLRP3 inflammasome, promoted similar responses. As with nigericin, 3 mM ATP treatment resulted in an inflammasome-dependent reduction of MTT conversion to formazan. Together, these results demonstrate that the NLRP3 inflammasome mediates membrane damage.

Nigericin alters mitochondrial function independently of NLRP3

To explore how inflammasome-activating stimuli impact mitochondrial function, we measured ATP levels in LPS-primed BMDM following nigericin exposure. Both WT and NLRP3$^{-/-}$ BMDM treated with nigericin contained reduced amounts of ATP compared with non-nigericin–treated cells, suggesting either decreased synthesis, increased consumption, or release of ATP into the culture supernatant (Fig. 2A). ATP levels in nigericin-treated cells were not preserved by coexposure to KCl, consistent with an NLRP3-independent event.

To further characterize nigericin-induced alterations in mitochondrial function, we used the Seahorse assay to measure OCR in WT and NLRP3$^{-/-}$ BMDM. Basal OCR levels in nonprimed WT and NLRP3$^{-/-}$ BMDM were comparable, whereas both showed reduced OCR levels 4 h after LPS priming. Nigericin rapidly increased OCR levels in both LPS-primed WT and LPS-primed NLRP3$^{-/-}$ BMDM, indicating a stress response in mitochondrial respiration (Fig. 2B, 2C). Following nigericin exposure, cells from both cell types were unable to respond to oligomycin or FCCP, which respectively inhibit ATP synthesis and uncouple electron transport. In contrast, LPS-primed WT or NLRP3$^{-/-}$ BMDM decreased OCR in response to oligomycin, followed by increased OCR in response to FCCP, which could be blocked by rotenone. These data show that LPS priming and nigericin each disrupt

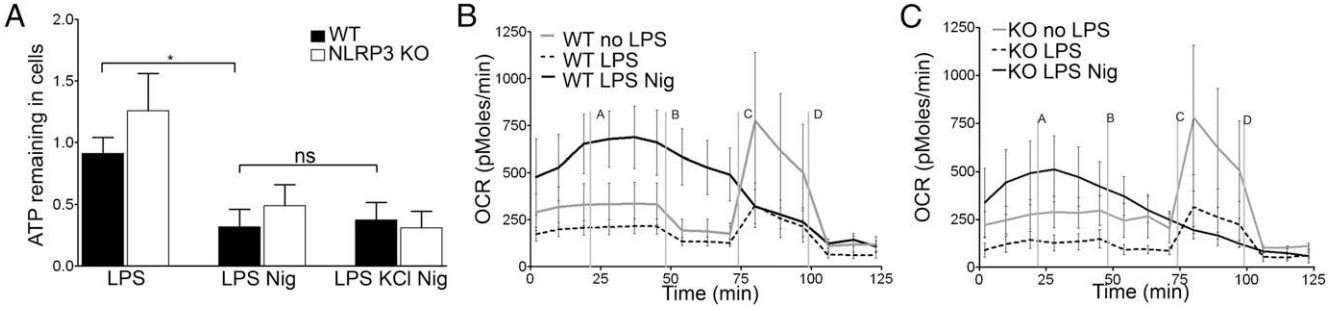

FIGURE 2. Loss of cellular ATP and decrease in OCR are NLRP3 independent. (**A**) WT or NLRP3$^{-/-}$ BMDM were LPS primed and treated with nigericin (Nig) for 30 min with or without KCl. Supernatants were collected and ATP levels measured. Error bars represent ± SD ($n \geq 6$, *$p = 0.0103$. ns, $p = 0.7941$). WT BMDM (**B**) or NLRP3$^{-/-}$ BMDM (**C**) were treated with Nig immediately before inserting the plate in the Seahorse machine. OCR was recorded as an average of three to four wells. Media (line A), oligomycin (line B), FCCP (line C), and rotenone (line D) were added as indicated. Error bars represent ± SD ($n = 4$, at 45 min. ns, $p = 0.3099$).

mitochondrial respiration in BMDM independently of NLRP3, with more severe dysfunction occurring after nigericin treatment. Taken together, these data demonstrate that nigericin reduces OCR and diminishes cellular ATP levels independently of NLRP3 in BMDM.

Loss of mitochondrial membrane integrity and cell death are NLRP3 dependent

Because WT and NLRP3$^{-/-}$ BMDM differ greatly in their ability to convert MTT through mitochondrial reductases (Fig. 1B), we further probed potential effects of NLRP3 on mitochondria using MitoTracker Red to measure membrane integrity. Using live-cell microscopy, we found that nigericin- or ATP-treated, LPS-primed WT and NLRP3$^{-/-}$ BMDM showed distinct differences in mitochondrial integrity (Fig. 3A–C, Supplemental Videos 1, 2). Approximately 30% of WT BMDM exhibited complete loss of mitochondrial integrity, whereas no loss was detected in NLRP3$^{-/-}$ BMDM in 1 h (Fig. 3D). In LPS-primed untreated or nonprimed nigericin-treated BMDM, no loss of mitochondrial integrity was seen (Fig. 3B, 3C). Furthermore, both nigericin- and ATP-induced MMP could be significantly reduced with exposure to KCl (Supplemental

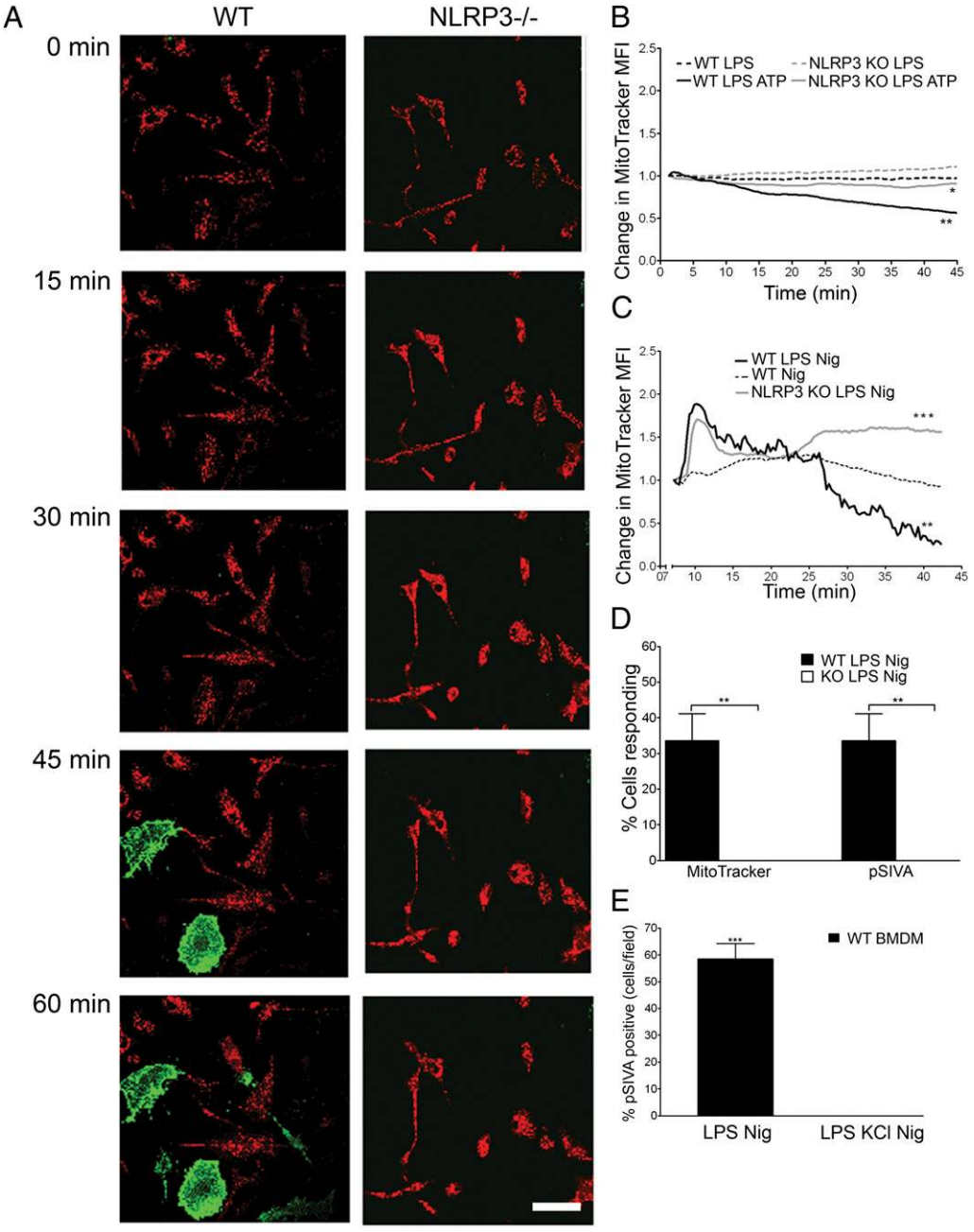

FIGURE 3. Loss of MMP and cell death are NLRP3 dependent. (**A**) WT and NLRP3$^{-/-}$ BMDM were LPS primed and treated with 20 μM nigericin. Cells were stained with MitoTracker red (red) and pSIVA (green) and imaged for 1 h with a confocal live-cell microscope. Images from one representative experiment shown. Scale bar, 50 μm. (**B**) Loss of MitoTracker red signal over time was recorded via live-cell microscopy. Cells were left untreated or treated with 3 mM ATP. Data were normalized to initial signal with background subtraction ($n \geq 9$, at 45 min. *$p = 0.0382$ for WT LPS ATP versus knockout [KO] LPS ATP, **$p = 0.0021$ for WT LPS versus WT LPS ATP). (**C**) Cells were imaged as in (B) with 20 μM nigericin (Nig; $n = 6$ at 40 min. **$p = 0.0015$, ***$p = 0.0001$). (**D**) Percentage of cells per field that lost MitoTracker signal or gained pSIVA signal over 1 h of confocal live-cell imaging. Error bars represent ± SD (MitoTracker, $n = 4$, **$p = 0.002$. pSIVA, $n = 3$, **$p = 0.002$). (**E**) Cells were treated with or without 50 mM KCl and imaged for 1 h on a confocal live-cell microscope. Percent of cells/field that were pSIVA positive at 60 min recorded. Error bars represent ± SD ($n = 3$. ***$p = 0.0001$). MFI, Mean fluorescence intensity.

Fig. 1A). Loss of mitochondrial membrane integrity correlated with exposure of phosphatidylserine (PS) at the plasma membrane (Fig. 3A, 3D). PS exposure was inhibited by the addition of KCl (Fig. 3E). These data demonstrate that NLRP3 inflammasome increases sensitivity of BMDM to loss of mitochondrial membrane integrity and subsequent cell death.

We investigated mtDNA localization in cells using PicoGreen, a dsDNA-specific dye that labels mitochondria and nuclei (20). We observed a decrease in mitochondrial PicoGreen staining in LPS-primed WT BMDM, but not in NLRP3$^{-/-}$ BMDM after 1 h exposure to nigericin (Supplemental Videos 3, 4). Loss of mtDNA in WT cells was prevented by KCl (data not shown) and coincided with loss of MitoTracker Red (Supplemental Video 3).

LMP precedes mitochondrial integrity breakdown during NLRP3 activation

A previously proposed model for NLRP3 activation suggested that following phagocytic uptake of indigestible particles known to trigger IL-1β secretion, rupture of phagolysosomes would release proteases into the cytosol, leading to assembly and activation of the NLRP3 inflammasome (7). We evaluated one aspect of this model using live-cell imaging. Lysosomes labeled with Lysotracker Green lose fluorescence within 15 min after exposure to nigericin in LPS-primed WT cells (Fig. 4A), consistent with either loss of lysosomal acidity or a loss of lysosomal membrane integrity in a process termed LMP. Labeled lysosomes in NLRP3$^{-/-}$ BMDM, however, retained fluorescence after nigericin treatment, demonstrating that LMP is NLRP3 dependent. LMP was also induced in WT, but not NLRP3$^{-/-}$ BMDM, by two other NLRP3 inflammasome activators, the pore-forming toxin TLO (Supplemental Fig. 1B) and ATP (data not shown). LMP always preceded MMP in both nigericin- and ATP-treated WT BMDM (Fig. 4B). In nigericin-treated cells, LMP occurred within 15 min of exposure to the stimulus, whereas MMP typically required between 30 and 60 min. In ATP-treated cells, LMP occurred within 10 min of exposure to the stimulus, and MMP typically required 15–30 min.

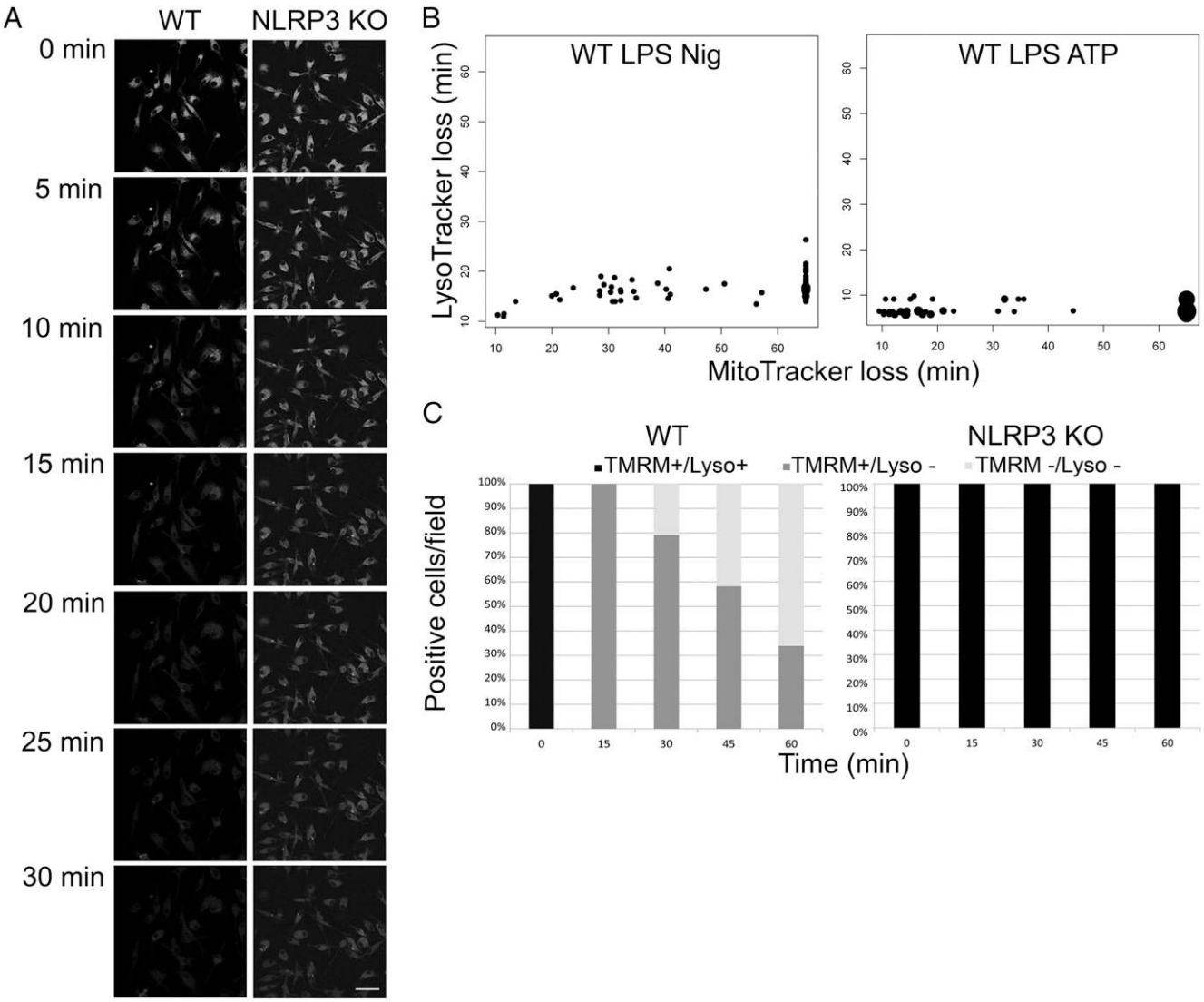

FIGURE 4. Loss of LMP is NLRP3 dependent. (**A**) WT and NLRP3$^{-/-}$ BMDM were LPS primed, stained with LysoTracker Green, and imaged via live-cell confocal microscope with 20 μM nigericin treatment for 30 min. Data from one representative experiment shown. Scale bar, 50 μm. (**B**) WT BMDM were LPS primed, treated with 20 μM nigericin (Nig) or 3 mM ATP, and stained with MitoTracker Red and LysoTracker Green. Cells were imaged for 1 h after Nig or ATP addition via live-cell microscopy. Data were recorded as time to loss of signal; each dot represents one cell, with larger dots representing multiple cells. Cells that did not lose MitoTracker Red were recorded as data points beyond 60-min imaging period. Data from five fields are displayed. (**C**) WT BMDM or NLRP3 knockout (KO) BMDM were LPS primed and Nig treated, stained with TMRM and LysoTracker Green (Lyso), and imaged with live-cell microscopy for 1 h. Percent of cells per field staining positive for each of the two dyes was recorded. $n \geq 5$ fields.

In addition, all WT BMDM exposed to nigericin underwent LMP, whereas on average, no >60–70% underwent MMP within 60 min (Fig. 4C). In contrast, NLRP3$^{-/-}$ BMDM did not undergo LMP or MMP with the 60-min experiment. LMP was blocked in WT BMDM by KCl, consistent with the NLRP3 dependence of the process (Supplemental Fig. 1C). Our results demonstrate that NLRP3 inflammasome activation results in loss of membrane integrity in lysosomes and mitochondria in kinetically distinct events.

IL-1β processing and secretion kinetically precedes loss of mitochondrial membrane integrity

A major function of the NLRP3 inflammasome in immunity is to regulate secretion of a family of nonconventionally secreted cytokines, including IL-1β. To probe the role of mitochondria and lysosomes in cytokine secretion, we performed kinetic analysis of processed IL-1β secretion. Processed IL-1β was detected in the supernatants of LPS-primed WT BMDM 15 min after nigericin exposure, and levels continued to increase over 30 min of nigericin exposure (Fig. 5A). Similar kinetics of IL-1β secretion were observed in LPS-primed ATP-treated WT BMDM (data not shown). Western blotting was used to confirm that released IL-1β was the cleaved biologically active form, not unprocessed precursor (Supplemental Fig. 2). IL-1β release was significantly decreased by addition of KCl 5 min after nigericin exposure, with progressively less inhibition occurring with KCl added at later times within the 30-min nigericin incubation period (Fig. 5B). Because LPS-primed, nigericin-exposed BMDM lose mitochondrial integrity and expose plasma membrane PS by ~30 min (Figs. 3, 4), this suggests that IL-1β secretion precedes cell death and MMP and correlates kinetically with LMP. LDH release occurred with nearly identical kinetics to IL-1β secretion and was also inhibited by KCl, consistent with compromised plasma membrane integrity before cell death (Fig. 5C, 5D).

IL-1β secretion distinct from organelle damage and cell death

To characterize the mechanisms underlying MMP, LMP, and IL-1β processing and secretion, we examined the requirement for caspase-1 in each process. Ac-YVAD-CMK (YVAD), a caspase-1 inhibitor, did not prevent the loss of lysosomal membrane integrity or mitochondrial membrane integrity in WT BMDM treated with nigericin (Fig. 6A). Furthermore, YVAD pretreatment blocked processing and secretion of IL-1β but did not significantly inhibit LDH release from WT BMDM (Fig. 6B, 6C). Although caspase-1 activity is required for the processing and secretion of mature IL-1β, it does not appear to be required in its active form to trigger LMP, MMP, or cell death.

We and others (7, 19) have shown the cathepsin B inhibitor CA-074 Me inhibits secretion of processed IL-1β. Cathepsin B is a lysosomal protease that is likely released during LMP. Because processing and secretion of IL-1β correlates kinetically with LMP (Figs. 4, 5), we tested whether cathepsin B participates in MMP. CA-074 Me did not inhibit LMP or MMP induced by nigericin in LPS-primed BMDM (Supplemental Fig. 3A). These results show that the role of NLRP3 inflammasome in IL-1β processing and secretion is distinct from effects on lysosomal and mitochondrial membrane integrity in its dependence on caspase-1 and cathepsin B.

NLRP3-dependent organelle damage and cytokine release is mediated by mitochondrial ROS

Next, we examined the potential role for mitochondrial ROS in IL-1β processing and secretion, LDH release, LMP, and MMP. Mito-Tempo, a mitochondria-specific ROS scavenger, reduced both IL-1β secretion after nigericin or ATP exposure (Fig. 6B) and LDH release after nigericin exposure in LPS-primed WT BMDM (Fig. 6C) (17). In addition, 500 μM Mito-Tempo also delayed LMP and reduced subsequent MMP in nigericin-treated WT BMDM (Fig. 6D, 6E, Supplemental Table I). Furthermore, LMP was significantly delayed and MMP reduced when ATP-exposed WT BMBM were treated with Mito-Tempo (Fig. 6E, Supplemental Fig. 3B). Together, these data suggest that mitochondrial ROS production is an early event that may lead to NLRP3 activation as well as inflammasome-dependent LMP, IL-1β secretion, MMP, and cell death.

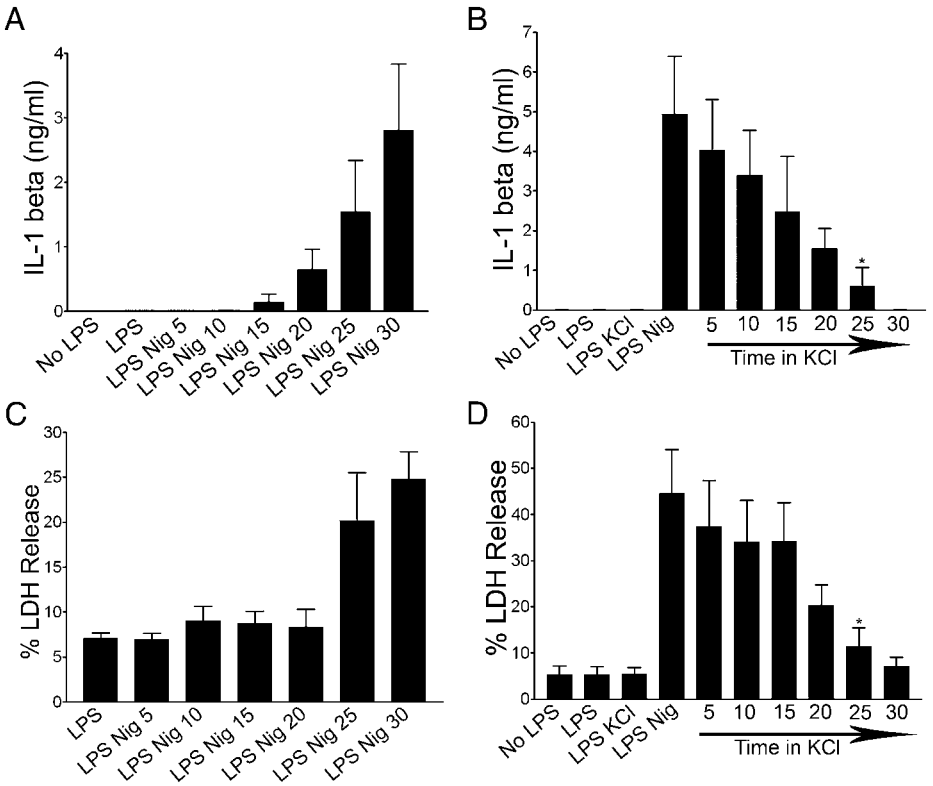

FIGURE 5. IL-1β processing and secretion is kinetically distinct from MMP. (**A**) WT BMDM were LPS primed or unprimed and treated with 20 μM nigericin (Nig) for 5–30 min. Supernatants were collected and analyzed for IL-1β using ELISA. Error bars represent ± SD; $n = 3$. (**B**) WT BMDM were treated with Nig for 30 min. A total of 50 mM KCl was added after 0–25 min following Nig treatment. Supernatants were collected and analyzed via IL-1β ELISA. Error bars represent ± SD; $n \geq 3$ (*p = 0.0294 for LPS Nig KCl 25 versus LPS Nig). WT BMDM were LPS primed and treated with Nig for 5–30 min (**C**) or were LPS primed and then had 50 mM KCl added 0–25 min following Nig treatment (**D**). Supernatants were collected for LDH release analysis. Data shown as percentage of LDH release by Triton X-100–treated control cells. Error bars represent ± SD; $n = 4$ (*p = 0.0475 for LPS Nig KCl 25 versus LPS Nig).

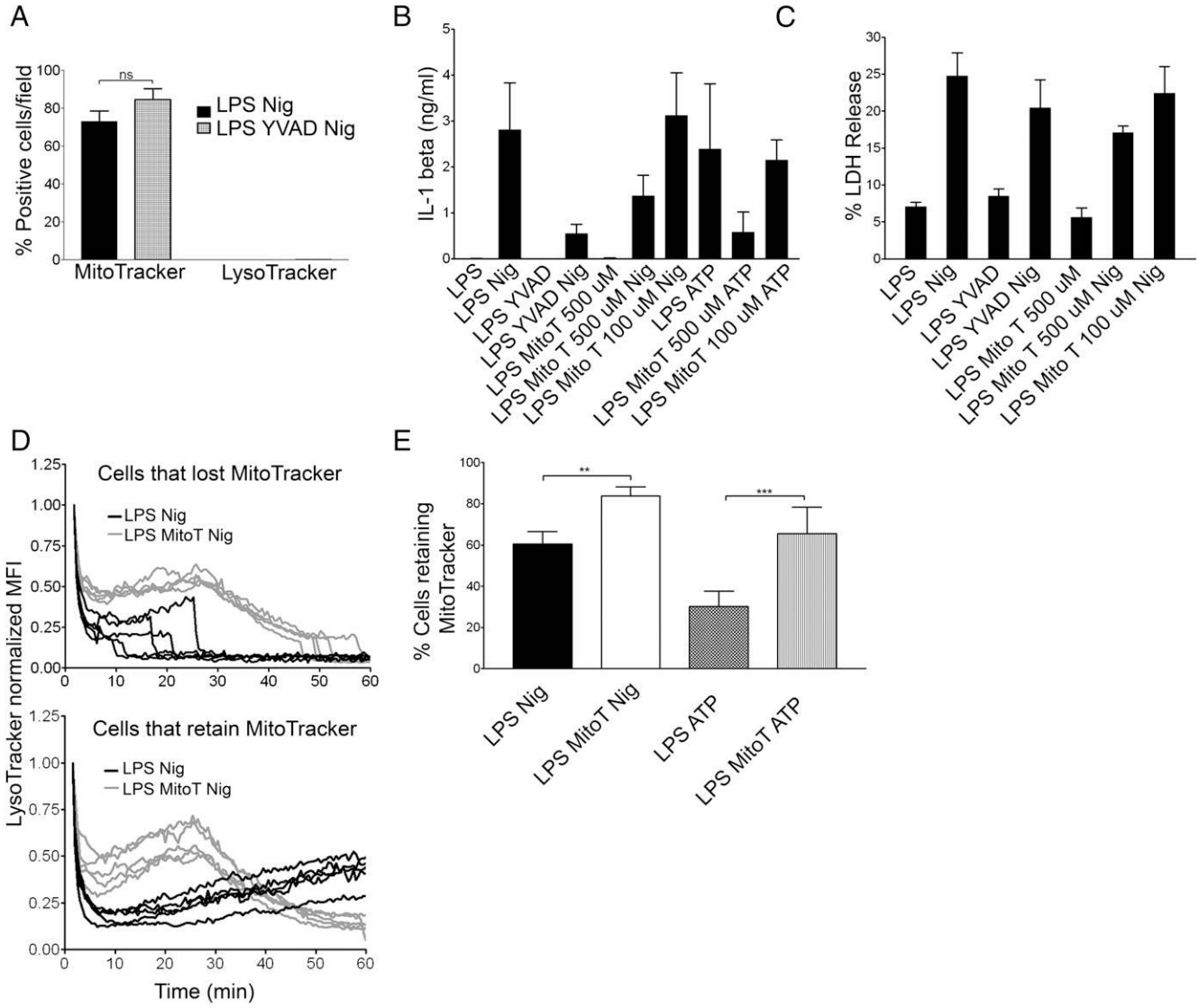

FIGURE 6. Mitochondrial ROS is required for NLRP3 inflammasome–dependent events. (**A**) WT BMDM were LPS primed, treated with nigericin (Nig) following YVAD exposure, and labeled with MitoTracker Red and LysoTracker Green. Cells were imaged via live-cell microscopy for 1 h. Data presented as positive cells per field at 60 min. Error bars represent ± SD; $n = 5$. WT BMDM were LPS primed and treated with Nig following 100 μM YVAD or 100 or 500 μM Mito-Tempo (MitoT). Supernatants were analyzed for IL-1β via ELISA (**B**) or LDH release (**C**) as percentage of LDH release by Triton X-100–treated control cells. Error bars represent ± SD; $n = 3$. (**D**) WT BMDM were LPS primed and Nig and 500 μM MitoT treated. LysoTracker and MitoTracker (not shown) mean fluorescence intensity (MFI) recorded via live-cell microscopy. The LysoTracker MFI was normalized to initial signal and background corrected. LysoTracker data are presented as one line per cell from five representative fields and split into two groups: cells that lost MitoTracker signal after 60 min of imaging (*top panel*) and cells that retained MitoTracker signal throughout the experiment (*bottom panel*). (**E**) WT BMDM were LPS primed and Nig or ATP treated with or without 500 μM MitoT. Cells were labeled with MitoTracker Red and imaged via live-cell microscopy. Data are presented as percent of cells per field retaining MitoTracker signal. Error bars represent ± SD; $n \geq 10$ fields (**$p = 0.0061$, ***$p < 0.0001$).

Discussion

Our results show that in addition to mediating processing and secretion of inflammatory cytokines, NLRP3 inflammasome influences the function and integrity of organelles, cell membrane permeability, and cell death. We examined the kinetics of these events at the single-cell level using live-cell microscopy in combination with biochemical assays in macrophages exposed to a prototypical NLRP3-activating stimulus. Our data suggest a multistep process of mitochondrial and lysosomal dysfunction and damage. Nigericin induces mitochondrial dysfunction and loss of cellular ATP independently of NLRP3 expression. The loss of cellular ATP was unaffected by addition of exogenous KCl, further supporting their NLRP3 independence. In WT but not NLRP3-deficient cells, lysosomal deacidification is observed and followed kinetically by loss of mitochondrial integrity (MMP) and exposure of PS on the cell surface. ROS derived from mitochondria appear to be responsible at least in part for the observed effects on lysosomes, termed LMP, because the ROS scavenger Mito-Tempo can delay both LMP and inhibit subsequent MMP. Both LMP and MMP can be inhibited in WT cells by exogenous KCl, which prevents the K^+ efflux required for NLRP3 activation. Based on these results in both nigericin-treated and ATP-treated cells, we propose a model in which some NLRP3 inflammasome activators induce mitochondrial and lysosomal damage, releasing soluble factors from these organelles that sequentially perpetuate inflammasome activation and cell damage. Although the exact kinetics

of these events differ between NLRP3 inflammasome activators, our data with two distinct stimuli suggest the sequence of events may remain the same. Our data strongly support a role for mitochondrial ROS released into the cytosol as one of these mediators, acting to induce LMP.

Inflammasome-mediated cell death is important for removal of cells infected with intracellular pathogens such as *Salmonella* (21). However, the most widely recognized functions of inflammasomes are to mediate extracellular release of IL-1 cytokine family members. Although we and others have been unable to visualize release of these cytokines from individual cells, IL-1β release can be detected in culture supernatants from WT cells by 15 min after nigericin exposure, which closely matches when LMP is first detected in nigericin-treated cells. This supports, but does not prove, a role for LMP in IL-1β secretion. Our data do not exclude the possibility that LMP could increase IL-1β release by inducing additional ROS release from mitochondria and further amplifying the cross-talk pathway with lysosomes (22). We found that when mitochondrial ROS production was inhibited with Mito-Tempo, both LMP and IL-1β secretion were reduced in ATP- and nigericin-treated cells. In contrast, we do not observe MMP and PS exposure in any cells until after IL-1β is readily detectable in culture supernatants, consistent with IL-1β release not requiring cell death.

Because LMP precedes MMP, it could be suggested that released lysosomal products directly damage mitochondria, resulting ultimately in cell death (15, 23). The identity of products from lysosomes that could destabilize mitochondria is unclear, but might be suggested to include ROS generated by Noxs in lysosomes, based on results reported in tumor cells (24). However, Nox1–4-deficient macrophages have been shown to produce normal levels of IL-1β, suggesting that lysosomal ROS is not required for NLRP3 inflammasome–dependent cytokine release (25, 26). An additional lysosomal product that might induce mitochondrial dysfunction is cathepsin B (27), which has been suggested to participate in NLRP3 inflammasome activation after its release from lysosomes into the cytosol in response to particulate inflammasome stimuli (7). Our data place NLRP3 activation upstream of LMP, which is inconsistent with this hypothesis, unless cathepsin B can be released from intact lysosomes. Although able to block IL-1β secretion, the cathepsin B inhibitor CA-074 Me had no effect on MMP. In summary, our data do not support a role for lysosomal products in inducing MMP, but do not exclude this possibility.

An important question raised by our experiments is how mitochondria and their products, including but not limited to ROS, can induce LMP in an NLRP3-dependent fashion. One possibility is suggested by a recent study showing that NLRP3 protein localized in the endoplasmic reticulum assembles with ASC bound to mitochondria and that this is mediated through microtubule-based movement of mitochondria (28). NLRP3 assembly might thus alter the distribution of mitochondria in the cell, bringing them into proximity with lysosomes, which can also be transported via microtubules (29). Lysosomes in WT but not NLRP3-deficient cells might then encounter higher concentrations of mitochondrial ROS or other released products, leading to selective damage and LMP.

In addition to ROS, mtDNA has been shown to activate the NLRP3 inflammasome (17). When we labeled mtDNA in BMDM with PicoGreen, we observed loss of signal from mitochondria in WT cells but no signal loss in NLRP3-deficient BMDM. The kinetics were identical to those seen for loss of MitoTracker Red in nigericin-treated cells, consistent with loss of mtDNA during MMP. This suggests that mtDNA is released from mitochondria largely after NLRP3 inflammasome is activated, although it does not exclude the possibility that small amounts of mtDNA could be released during initial mitochondrial dysfunction.

Our results show that both LMP and MMP in BMDM do not require active caspase-1, because they each are unaffected by the inhibitor YVAD. We have conducted preliminary experiments with BMDM from caspase-1–deficient mice and see partial inhibition of MMP. However, these mice also lack caspase-11, which plays a role in cell death, clouding interpretation of this data (30–32). Because YVAD blocks caspase-1 cleavage, uncleaved caspase-1 could potentially mediate cell death, as shown for AIM2 and NLRC4 inflammasomes (5). However, NLRP3 lacks the caspase activation and recruitment domain needed to directly recruit uncleaved caspase-1.

NLRP3 inflammasome assembles at the endoplasmic reticulum–mitochondrial interface (28, 33), the site where autophagosomes have been recently shown to form in nonimmune cells (34). Inhibition of autophagy or mitochondrial autophagy (mitophagy) have been shown to increase IL-1β secretion in macrophages, perhaps through the accumulation of damaged mitochondria, leading to elevation of cytosolic ROS levels (35–37). Although precisely how IL-1 family cytokines are packaged for secretion remains unclear, we speculate that autophagy might interfere with packaging of IL-1β into specialized secretory vesicles also originating from this site.

Acknowledgments

We thank the present and past members of the Salter laboratory, especially Jessica Chu, L. Michael Thomas, and Chengqun Sun. WT or NLRP3$^{-/-}$ bone marrow was provided by Lisa Borghesi, Timothy Billiar, Olivera Finn, Robert Binder, Gabriel Nuñez, and Richard Flavell (Howard Hughes Medical Institute). The Center for Biological Imaging provided reagents, technical support, and advice, especially Greg Gibson and Salony Maniar. We also thank the laboratory of Lawrence Kane for the use of the luminometer. Catherine Corey provided technical assistance with the Seahorse assay.

Disclosures

The authors have no financial conflicts of interest.

References

1. Pétrilli, V., C. Dostert, D. A. Muruve, and J. Tschopp. 2007. The inflammasome: a danger sensing complex triggering innate immunity. *Curr. Opin. Immunol.* 19: 615–622.
2. Agostini, L., F. Martinon, K. Burns, M. F. McDermott, P. N. Hawkins, and J. Tschopp. 2004. NALP3 forms an IL-1beta-processing inflammasome with increased activity in Muckle-Wells autoinflammatory disorder. *Immunity* 20: 319–325.
3. Dubyak, G. R. 2012. P2X7 receptor regulation of non-classical secretion from immune effector cells. *Cell. Microbiol.* 14: 1697–1706.
4. Miao, E. A., J. V. Rajan, and A. Aderem. 2011. Caspase-1-induced pyroptotic cell death. *Immunol. Rev.* 243: 206–214.
5. Broz, P., J. von Moltke, J. W. Jones, R. E. Vance, and D. M. Monack. 2010. Differential requirement for Caspase-1 autoproteolysis in pathogen-induced cell death and cytokine processing. *Cell Host Microbe* 8: 471–483.
6. Bauernfeind, F., A. Ablasser, E. Bartok, S. Kim, J. Schmid-Burgk, T. Cavlar, and V. Hornung. 2011. Inflammasomes: current understanding and open questions. *Cell. Mol. Life Sci.* 68: 765–783.
7. Hornung, V., F. Bauernfeind, A. Halle, E. O. Samstad, H. Kono, K. L. Rock, K. A. Fitzgerald, and E. Latz. 2008. Silica crystals and aluminum salts activate the NALP3 inflammasome through phagosomal destabilization. *Nat. Immunol.* 9: 847–856.
8. Halle, A., V. Hornung, G. C. Petzold, C. R. Stewart, B. G. Monks, T. Reinheckel, K. A. Fitzgerald, E. Latz, K. J. Moore, and D. T. Golenbock. 2008. The NALP3 inflammasome is involved in the innate immune response to amyloid-beta. *Nat. Immunol.* 9: 857–865.
9. Newman, Z. L., S. H. Leppla, and M. Moayeri. 2009. CA-074Me protection against anthrax lethal toxin. *Infect. Immun.* 77: 4327–4336.
10. Dostert, C., G. Guarda, J. F. Romero, P. Menu, O. Gross, A. Tardivel, M. L. Suva, J. C. Stehle, M. Kopf, I. Stamenkovic, et al. 2009. Malarial hemozoin is a Nalp3 inflammasome activating danger signal. *PLoS ONE* 4: e6510.

11. Zhou, R., A. Tardivel, B. Thorens, I. Choi, and J. Tschopp. 2010. Thioredoxin-interacting protein links oxidative stress to inflammasome activation. *Nat. Immunol.* 11: 136–140.
12. Latz, E. 2010. NOX-free inflammasome activation. *Blood* 116: 1393–1394.
13. Sorbara, M. T., and S. E. Girardin. 2011. Mitochondrial ROS fuel the inflammasome. *Cell Res.* 21: 558–560.
14. Green, D. R., and G. Kroemer. 2004. The pathophysiology of mitochondrial cell death. *Science* 305: 626–629.
15. Boya, P., K. Andreau, D. Poncet, N. Zamzami, J. L. Perfettini, D. Metivier, D. M. Ojcius, M. Jäättelä, and G. Kroemer. 2003. Lysosomal membrane permeabilization induces cell death in a mitochondrion-dependent fashion. *J. Exp. Med.* 197: 1323–1334.
16. Martinon, F. 2012. Dangerous liaisons: mitochondrial DNA meets the NLRP3 inflammasome. *Immunity* 36: 313–315.
17. Nakahira, K., J. A. Haspel, V. A. Rathinam, S. J. Lee, T. Dolinay, H. C. Lam, J. A. Englert, M. Rabinovitch, M. Cernadas, H. P. Kim, et al. 2011. Autophagy proteins regulate innate immune responses by inhibiting the release of mitochondrial DNA mediated by the NALP3 inflammasome. *Nat. Immunol.* 12: 222–230.
18. Shimada, K., T. R. Crother, J. Karlin, J. Dagvadorj, N. Chiba, S. Chen, V. K. Ramanujan, A. J. Wolf, L. Vergnes, D. M. Ojcius, et al. 2012. Oxidized mitochondrial DNA activates the NLRP3 inflammasome during apoptosis. *Immunity* 36: 401–414.
19. Chu, J., L. M. Thomas, S. C. Watkins, L. Franchi, G. Núñez, and R. D. Salter. 2009. Cholesterol-dependent cytolysins induce rapid release of mature IL-1beta from murine macrophages in a NLRP3 inflammasome and cathepsin B-dependent manner. *J. Leukoc. Biol.* 86: 1227–1238.
20. Ashley, N., D. Harris, and J. Poulton. 2005. Detection of mitochondrial DNA depletion in living human cells using PicoGreen staining. *Exp. Cell Res.* 303: 432–446.
21. Miao, E. A., I. A. Leaf, P. M. Treuting, D. P. Mao, M. Dors, A. Sarkar, S. E. Warren, M. D. Wewers, and A. Aderem. 2010. Caspase-1-induced pyroptosis is an innate immune effector mechanism against intracellular bacteria. *Nat. Immunol.* 11: 1136–1142.
22. McGuire, K. A., A. U. Barlan, T. M. Griffin, and C. M. Wiethoff. 2011. Adenovirus type 5 rupture of lysosomes leads to cathepsin B-dependent mitochondrial stress and production of reactive oxygen species. *J. Virol.* 85: 10806–10813.
23. Boya, P., R. A. Gonzalez-Polo, D. Poncet, K. Andreau, H. L. Vieira, T. Roumier, J. L. Perfettini, and G. Kroemer. 2003. Mitochondrial membrane permeabilization is a critical step of lysosome-initiated apoptosis induced by hydroxychloroquine. *Oncogene* 22: 3927–3936.
24. Kroemer, G., and M. Jäättelä. 2005. Lysosomes and autophagy in cell death control. *Nat. Rev. Cancer* 5: 886–897.
25. van Bruggen, R., M. Y. Köker, M. Jansen, M. van Houdt, D. Roos, T. W. Kuijpers, and T. K. van den Berg. 2010. Human NLRP3 inflammasome activation is Nox1-4 independent. *Blood* 115: 5398–5400.
26. Dostert, C., V. Pétrilli, R. Van Bruggen, C. Steele, B. T. Mossman, and J. Tschopp. 2008. Innate immune activation through Nalp3 inflammasome sensing of asbestos and silica. *Science* 320: 674–677.
27. Li, Z., M. Berk, T. M. McIntyre, G. J. Gores, and A. E. Feldstein. 2008. The lysosomal-mitochondrial axis in free fatty acid-induced hepatic lipotoxicity. *Hepatology* 47: 1495–1503.
28. Misawa, T., M. Takahama, T. Kozaki, H. Lee, J. Zou, T. Saitoh, and S. Akira. 2013. Microtubule-driven spatial arrangement of mitochondria promotes activation of the NLRP3 inflammasome. *Nat. Immunol.* 14: 454–460.
29. Bálint, S., I. Verdeny Vilanova, A. Sandoval Álvarez, and M. Lakadamyali. 2013. Correlative live-cell and superresolution microscopy reveals cargo transport dynamics at microtubule intersections. *Proc. Natl. Acad. Sci. USA* 110: 3375–3380.
30. Aachoui, Y., I. A. Leaf, J. A. Hagar, M. F. Fontana, C. G. Campos, D. E. Zak, M. H. Tan, P. A. Cotter, R. E. Vance, A. Aderem, and E. A. Miao. 2013. Caspase-11 protects against bacteria that escape the vacuole. *Science* 339: 975–978.
31. Case, C. L., L. J. Kohler, J. B. Lima, T. Strowig, M. R. de Zoete, R. A. Flavell, D. S. Zamboni, and C. R. Roy. 2013. Caspase-11 stimulates rapid flagellin-independent pyroptosis in response to *Legionella pneumophila*. *Proc. Natl. Acad. Sci. USA* 110: 1851–1856.
32. Shin, S., and I. E. Brodsky. 2013. Caspase-11: the noncanonical guardian of cytosolic sanctity. *Cell Host Microbe* 13: 243–245.
33. Zhou, R., A. S. Yazdi, P. Menu, and J. Tschopp. 2011. A role for mitochondria in NLRP3 inflammasome activation. *Nature* 469: 221–225.
34. Hamasaki, M., N. Furuta, A. Matsuda, A. Nezu, A. Yamamoto, N. Fujita, H. Oomori, T. Noda, T. Haraguchi, Y. Hiraoka, et al. 2013. Autophagosomes form at ER-mitochondria contact sites. *Nature* 495: 389–393.
35. Naik, E., and V. M. Dixit. 2011. Mitochondrial reactive oxygen species drive proinflammatory cytokine production. *J. Exp. Med.* 208: 417–420.
36. Saitoh, T., N. Fujita, M. H. Jang, S. Uematsu, B. G. Yang, T. Satoh, H. Omori, T. Noda, N. Yamamoto, M. Komatsu, et al. 2008. Loss of the autophagy protein Atg16L1 enhances endotoxin-induced IL-1beta production. *Nature* 456: 264–268.
37. Shi, C. S., K. Shenderov, N. N. Huang, J. Kabat, M. Abu-Asab, K. A. Fitzgerald, A. Sher, and J. H. Kehrl. 2012. Activation of autophagy by inflammatory signals limits IL-1β production by targeting ubiquitinated inflammasomes for destruction. *Nat. Immunol.* 13: 255–263.